

## Experimental Evaluation of Shape Memory Alloy Characteristics

Hussein M. Alalem

School of Engineering & Applied Science, The Libyan Academy, Tripoli, Libya

### Abstract

The paper concerns a body of research into the properties and behaviour of the shape memory alloys (SMA). Test rigs were designed and constructed leading to the determination of the SMA material temperature, resistance and displacement characteristics. Indirect temperature measurements showed accurate and reliable SMA wire temperatures with all its boundaries. Isothermal loading and unloading and shape recovery force measurements were performed to characterise parameters governing the phase transformation of the SMA material in terms of stress, strain behaviour and the effect of stress on the SMA temperature. Results showed transformation temperatures of the SMA are stress dependent parameters, they are different under different stress. The technology employed utilizes a 100 $\mu$ m diameter heat actuated wire of Nickel-Titanium (NiTi) shape-memory alloy (SMA) which contracts when pulsed with an electrical current (in effect heating the metal) under pre-stress.

**Keywords:** SMA, Temperature, Resistance, Displacement, Force, Stress, Strain, Austenite, Martensite.

### Introduction

After the excellent shape memory properties of a titanium-nickel alloy (NiTi) were announced in 1965, intensive investigations have been made to elucidate the mechanics of its basic behavior. Practical development accelerated even further and the study of shape memory alloys has continued at an increasing pace since and more products using these materials are coming to the market each year. Shape Memory Alloys (SMA's) are novel materials that demonstrate the ability to return to some previously defined shape or size when subjected to the appropriate thermal procedure [1]. Generally, these materials can be plastically deformed at some relatively low temperature, and upon exposure to some higher temperature will return to their shape prior to the deformation. In other words, if the alloy is mechanically deformed in its martensitic (low temperature) phase and then heated it is transformed into the memorized austenitic shapes. SMA materials can directly convert thermal energy to mechanical work [2]. This phenomenon, which provides a unique mechanism for actuation, is associated with the unique interaction between the martensite and austenite crystal structures of the SMA material. These alloys exhibit the so-called mechanical-memory effect caused by a structural transition between a martensitic phase and an austenitic phase, characterized by higher crystalline symmetry. This transition starts when the alloy is heated past its austenitic start temperature and ends upon reaching the austenitic finish temperature [3]. Materials that exhibit shape memory only upon heating are referred to as having a one way shape memory. Some materials also undergo a change in shape upon re-cooling [4]. These materials have a two-way shape memory. Although a relatively wide variety of alloys are known to exhibit the shape memory effect, only those that can recover substantial amounts of strain or that generate significant force upon changing shape are of commercial interest. It has now been over 70 years [5] since the first observations of shape memory and the practical development of shape memory alloys took place. According to Otsuka and Wayman (1998) [6], the first reported steps towards the discovery of the shape memory effect were taken in the 1930s and over 30 years elapsed before

people first began to find applications for such effect and noted the reversibility of the transformation in a AuCd (gold-cadmium) alloy by metallographic observations and resistivity changes. This phenomenon of transformation [3] is caused by the interaction in the crystal lattice of the crystalline structure of the material that is activated through changes in temperature and/or loading. Ölander [7] discovered the so called pseudoelastic behaviour of the AuCd alloy in 1932. This effect of pseudoelasticity which is similar to any elastic behaviour occurs when a mechanical load is applied on the SMA material at a temperature above the transformation level causing deformation on the material. When the load is removed, the deformation is then disappears causing a very large recoverable deformations [8]. However, it was not until 1962 that Buehler and co-workers at the U.S. Naval Ordnance Laboratory discovered the effect in equiatomic nickel-titanium (NiTi), which can be considered a breakthrough in the field of shape memory materials, [1], [5]. In this work several experimental test rigs were implemented to investigate the properties of SMA. An oil bath test-rig was designed to provide indirect temperature measurements for an SMA wire. A test rig for determining the effect of stress on the SMA wire strain and resistance was also designed. Finally an experiment was performed to measure the dynamic performance of the SMA tactile sensor using a laser sensing measurement technique.

## Experimental Methods

**Indirect Temperature Measurements.** Getting accurate and reliable temperature measurement of the NiTi SMA wire directly using a thermocouple is almost impossible. Since the surface of the SMA wire is very small ( $\text{Ø}100\mu\text{m}$ ). The conventional temperature measurement with a thermocouple clamped on the SMA wire is proved not accurate and failed to provide a proper measurement since a lot of heat loss was occurred. For this reason, an indirect temperature measurement was seen as an alternative and a better measurement method in such conditions. In order to obtain a proper temperature measurement, an accurate measurement method has to be developed and tested to measure the temperature of such a wire of a diameter of  $\text{Ø}100\mu\text{m}$ , thus models can be validated with respect to the estimated and measured temperatures. Fig. 1 shows the experimental set up of the oil bath experiment which was designed for the indirect temperature measurement for the 100 micro meters NiTi SMA wire.

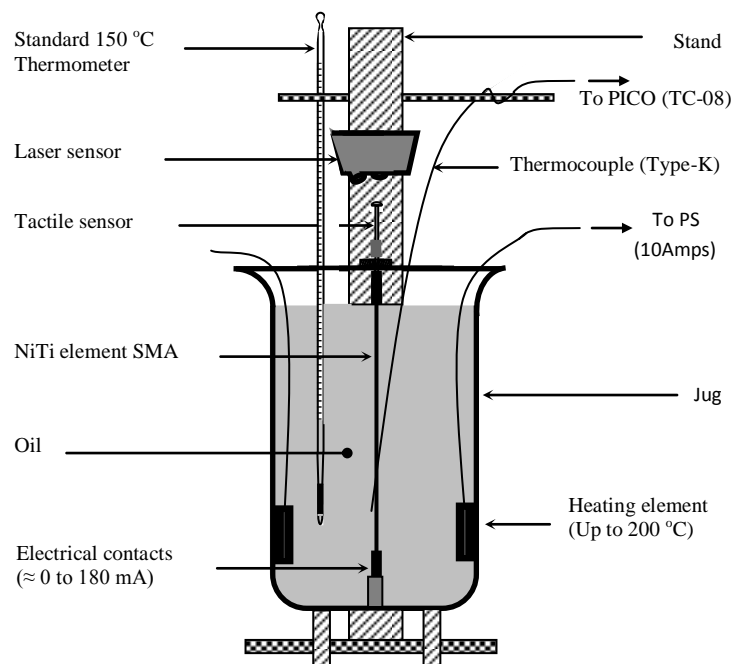


Fig. 1. Scheme of temperature measurement oil bath setup

The apparatus of the experiment consist of a 3-litre capacity high temperature oil-bath based jug of 0.2 mm diameter and 40 mm height mounted on a stand. The 115 mm long NiTi wire arrangement is immersed in

the centre of the oil bath. Two aluminium housed power wire-wound resistors of a maximum hot spot of up to 200 °C acting as electric heating source are attached to each of the side walls of the jug. The heating source is connected to a stabilized power supply (approximately 1.5 W). Heat transfer from the heaters to the SMA wire is due to the cumulative effect of different transfer mechanisms [4]. The heat transfer from the heaters to the wire causes temperature changes. A type K thermocouple of exposed welded junction is attached to a slider within the stand and immersed in the oil bath alongside the SMA wire. The thermocouple is used to measure the wire temperature at any position. A standard 150 °C Thermometer BS170/51 (100 mm immersion) was immersed alongside the NiTi wire in the oil bath to measure the oil temperature acting as a second means of temperature measurement. The purpose of this thermometer is to monitor the oil temperature, and to ensure a true reading of the oil temperature when compared with the thermocouple temperature reading if differed. The temperature of the SMA wire was measured using the PICO TC-08 type data logger in conjunction with type K thermocouple. The data logger includes all the electronics required to convert the measured parameter to a linear voltage of 10mV°C with an accuracy of  $\pm 0.3\%$  and 0.5 °C. It has an input range of  $\pm 70$  mV with 20 bits resolution [9]. The TC-08 data logger requires a relatively stable power voltage of between 4 and 30 v. It uses PicoLog data acquisition powerful software for collecting, analyzing and displaying data.

**Optoelectronic Displacement Measurement.** Micro-Epsilon, OptoNCDT 1605 laser sensor with analog signal processing was used to measure the displacement of the tactile sensor during the oil bath experiment. This optical sensor measures movement along the axis of the laser beam reflecting off a target surface perpendicular to that beam. The laser sensor measures the pin movement with high precision and sensitivity 5.0V/mm [10] and without contact against the tactile element surface. The Micro-Epsilon laser sensor is attached on top of the frame box facing the sensor head and mounted rigidly to the case so that it truly measures displacement of the pin. The measured values of the pin deflection which reflects the SMA wire strain were recorded using the PICO ADC-11 data acquisition type of input range of 0 to 2.5V with 10 bits resolution [9]. This was used with a considerable accuracy to record the measured displacement from the oil bath experiment. The laser sensor uses the triangulation measuring principle to give a very accurate measurement of the tactile element deflection. A point of light is projected from the optical sensor onto the top end of the tactile element and reflected diffusely. This point is focused on a position sensitive device by a lens. Fig. 2 shows the position sensitive element supplies a position dependent, analog output voltage proportional to the measuring distance between the laser sensor and the tactile element. The output is a linear analog voltage of (+/- 10 V) corresponding to the displacement range of the tactile element, with a sensitivity of 5.0V/mm.

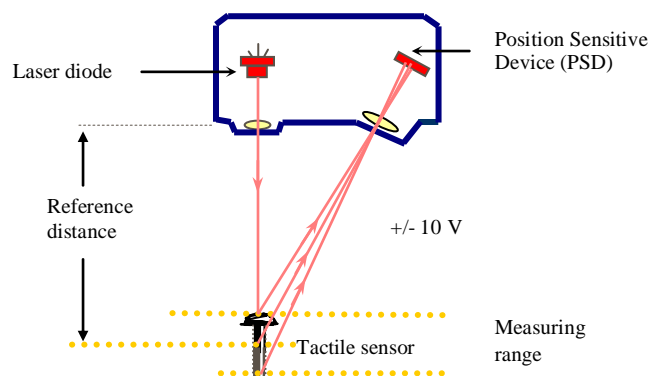


Fig. 2. Triangulation measuring principle

**Mechanism of SMA Measurement.** The mechanical properties of the SMA depend on many variables. The experimental work here is focused mainly on the response of the SMA to the loading paths in a quasi-plastic domain where the deformation mechanism is dominantly governed by the stress-induced martensitic transformation. We will study the stress-strain behaviour and the effect of stress on the electrical resistance

of the wire. One sample of  $\text{Ø}100\mu\text{m}$  NiTi SMA wire was used in this experiment work and subjected to various loading paths in tension. The SMA wire has a length of 100 mm. It is arranged as shown in the schematic illustration of the test bed in Fig. 3.

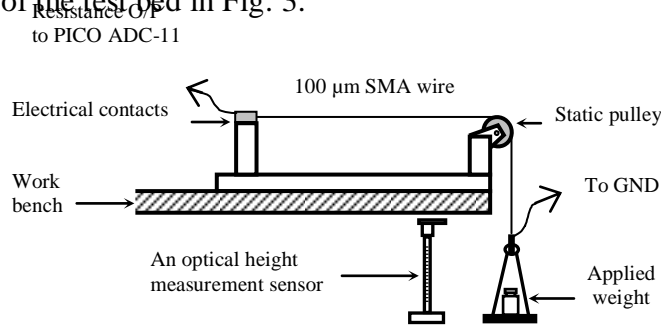


Fig. 3. Schematic of the test bed

The wire was attached to a rigid wooden frame at one end and passed over a pulley then attached to a weight hanger of 100 grams at the other. The reason for using a pulley was to substantially eliminate the effects of any sliding friction between the wire and wooden frame. The wooden frame is rigidly fixed to a bench to provide the necessary support to the mass hanger when force is applied. The load was applied using a selection of weights of 50 and 100grams i.e. a total mass of 500 grams, producing enough force of 4.85 N. The PICO ADC-11 data logger was used to record the measured wire resistance and displacement.

**Detecting Force Applied.** A test was performed to detect the tactile response when a known force is applied. The method used for applying force on the tactile sensor is shown in Fig. 4. A meter plate was placed on top of the tactile sensor. The plate was attached un-riveted at point  $P_2$  to ensure that friction is almost zero. Weight was applied on the plate at the centre point between  $P_1$  and  $P_2$ , note that the distance between  $L_1$  and  $L_2$  should be equal which means that the distance between points  $W$  and  $P_2$  is equal to the distance between points  $W$  and  $P_1$ . The tactile pin deflection was monitored by the Micro-Epsilon, optoNCDT 1605 laser sensor.

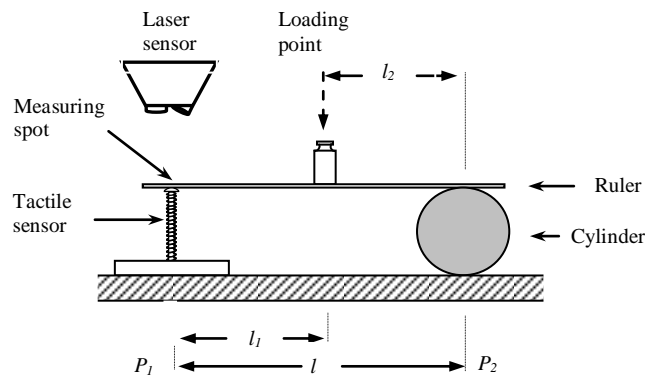


Fig. 4. Measurement of applied force on tactile

Forced cooling condition was applied and loads of up to 255 grams at 15 grams increments were used. The force exerted on the tactile sensor is determined by the following relationship:

$$W_1g = P_1l$$

$$P_1 = [(W_1/l) + (1/2mr)]g$$

where  $W$  is the applied mass in grams,  $l$  is the length of ruler in mm,  $P_l$  is the point where the actual weight is to be measured,  $m_r$  is the ruler mass and  $g$  is the gravity.

**Results**

**Martensitic Transformation and Hysteresis.** The plot in Fig. 5 extracted from the indirect temperature measurement experiment (oil bath) represents the elongation effect of the SMA wire during heating and convection cooling.

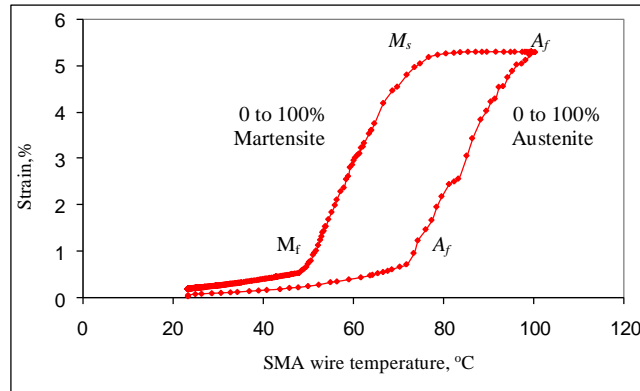


Fig. 5. Transformation versus temperature curve for the 100µm NiTi wire

The Micro-Epsilon laser sensor was used to measure the length variations of the wire, and data were recorded and treated by the PICO-11 data logger. The temperature of the wire was measured indirectly by type K thermocouple. The measured temperature readings were recorded by the TC-08 data logger. The testing rig using oil bath jug allows controlling also the minimum and maximum temperatures of the wire, so that it is possible to realize partial transformation. From Fig. 5 the strain induced by the tactile sensor tip deflection is plotted versus temperature. The deflection is almost zero until the transformation starts. The deflection increases with temperature and martensite fraction  $\zeta_M$  in the SMA layer decreases. The deflection comes to its steady condition when the SMA wire becomes completely austenite  $A_s$  at 100%. On cooling however, the deflection will decrease with temperature causing the martensite fraction  $\zeta_M$  in the SMA layer to increase. The deflection comes to an end when the SMA wire becomes completely martensite  $M_f$  at 100%. Fig. 6 shows that, the temperature range for the martensite-to-austenite transformation, i.e. soft-to-hard transition that takes place upon heating is somewhat higher than that for the reverse transformation upon cooling. The difference between the transition temperatures upon heating and cooling is the well known hysteresis effect.

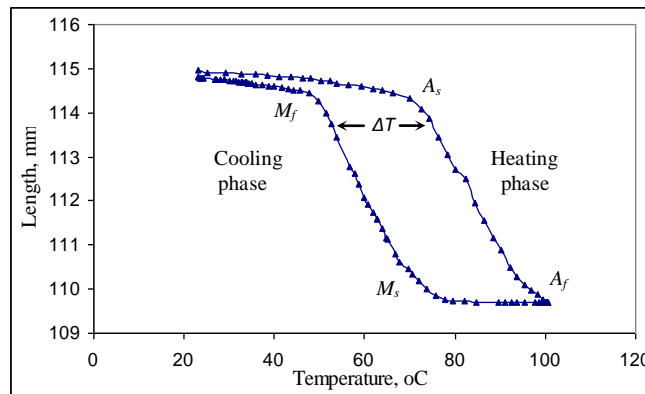


Fig. 6. Wire motion and temperature showing martensitic transformation and hysteresis

This hysteresis is generally the difference between the temperatures at which the material is 50 % transformed to austenite upon heating and 50 % transformed to martensite upon cooling. This difference can be up to 20-30 °C. In practice, this means that an alloy designed to be completely transformed by body temperature upon heating  $A_f < 37$  °C would require cooling to about +5 °C to fully retransform into martensite  $M_f$ .

**Temperature and Resistance Relationship.** Fig. 7 shows an experimental result plot of resistance versus temperature that was extracted from the oil bath experiment. The purpose of the test was to observe the variation in the SMA-wire resistance when heat is applied. The Ø100 µm NiTi wire had an initial resistance of approximately 19 Ω. As the wire is heated from cold, it begins to transform into the austenite phase at the austenite start temperature  $A_s$  where the resistance of the wire drops almost immediately from 19 Ω to around 15.5 Ω, and the transformation is essentially complete at the austenite finish temperature  $A_f$ . Likewise, as the hot wire is cooled, it transforms back into the martensite phase between the martensite start and finish temperatures  $M_s$  and  $M_f$ . These temperatures are lower than those for the heating curve, because of thermal hysteresis in the transformation.

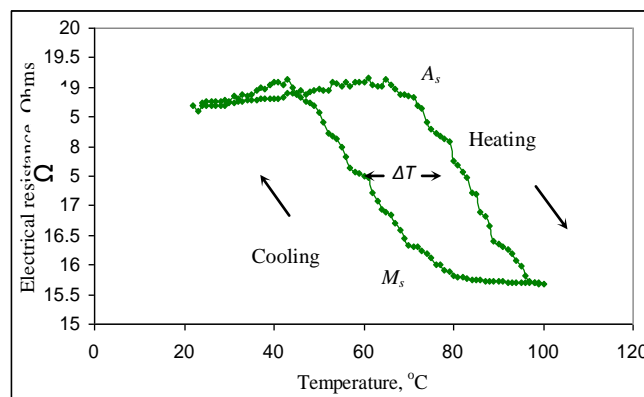


Fig. 7. NiTi wire electric resistance versus temperature  
With indication of the phase transformation temperatures

It can be seen from the plot that the resistance behaviour is very nonlinear. The phase transformation from the martensite phase to the austenite phase had a little influence on the electrical resistance. The phase transformation within the austenite phase .i.e. from  $A_s$  to  $A_f$  greatly decreased the electrical resistance. Furthermore, the phase transformation within the martensite phase .i.e. from  $M_s$  to  $M_f$  greatly increased the electrical resistance. This means that, controlling the wire is very difficult task. However, it can be possible to use the resistance for a bi-stable controller to go full martensite to full austenite. This can be recommended for further work.

**SMA Stress-strain Mechanism.** Martensitic transformations in SMA are due macro- scopically to a pseudo-sharing deformation, and therefore operate as a deformation mode similar to slip or twinning in ordinary metals and alloys under stress. However, since martensitic transformations involve a characteristic of reverse transformations, which are absent in deformation by slip or twinning, the deformation alloys which undergo martensitic transformations is remarkably different from ordinary metals and alloys. In other words, there is a marked variation of mechanical behaviour of SMA at different temperatures. Fig. 8 contains SMA stress-strain curves tensile-tested at various temperatures, extracted from series of tests performed on a 100 µm NiTi SMA wire using the test bed described in Fig. 3. The stress – strain curves

describe the tensile loading and unloading behaviour of the Ni-Ti wire, which has undergone various temperatures of impulsive Joule heating, and air convection cooling. The wire was heated by Joule heating, and then after reaching a certain temperature, the wire was slowly left to cool in an ambient temperature (free air convection). Stress was then applied in a form of load increments. The stress-strain curves in Fig. 8 show a characteristic feature in which the shapes of the curves very significantly depend upon the relation between the characteristic transformation temperatures of the SMA wire (i.e.  $M_s$ ,  $M_f$ ,  $A_s$ , and  $A_f$ ) and the test temperature  $T$ . The curves can be divided into three regions AB, BC and CD. When sufficient stress is applied, the first region AB shows the martensitic structure behaves in a detwinning type of mechanism. It will start to yield and detwin as the grains reorient such that they are all aligned in the same direction. It is to be noted that, the modulus and elastic limit of the wire increase with the increase in temperature causing large strain of approximately 5% to 8% due to phase transformation. However this strain does not appear in curves of the specimen when it was pre-heated at 20 °C and 40 °C temperatures (i.e.  $T < A_s$ ) as the specimen had still not reached the phase transformation region. The second region BC is usually linear but not purely elastic and takes place at a higher stress. It provides heat recoverable plastic strains of detwinned martensite. In the third region CD, during unloading, there is an onset of irrecoverable plastic strains similar to conventional metals. We can now conclude that, as the heat processing temperature gets higher the amount of recoverable strain becomes larger. Also, the transformation temperatures of the wire are stress dependent parameters, i.e., they are different under different loads. i.e. the variation of wire deflection on cooling or heating is proportional to the amount of martensite.

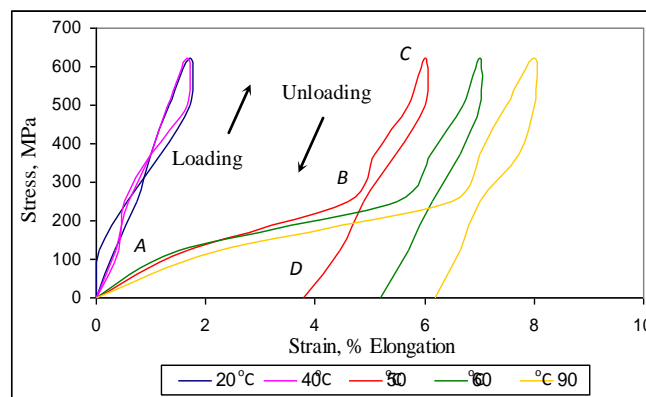


Fig. 8 Stress-strain behaviour of NiTi SMA wire for the martensite phase

**SMA Stress-Resistance Behavior under Tensile Loading.** Shape memory alloy exhibits the so-called mechanical memory effect. This is caused by a structural transition between a martensitic phase and an austenitic phase, characterized by higher crystalline symmetry. During the course of the shape recovery, the SMAs produce a combination of both force and displacement. The amount of force and displacement is dependent on the exact geometry of the SMA wire and the amount of heating [11]. Here we explore one of the measurements that have been used to observe the variation of electrical resistance during some thermo-mechanic procedures. It is an attempt to measure the effect of tensile stress on the NiTi wire electrical resistance. A NiTi SMA wire was tested in the test bed described in Fig. 3. The wire was heated by Joule heating of various heating pulses, and it was tensile loaded up to 500 MPa. The tensile test was carried out while maintaining the wire temperature constant by keeping the wire energized at one particular heating pulse for every cycle test. The variation of the electrical resistance is simultaneously measured during this procedure. From Fig. 9 at the heating pulses between 0.06W and 0.24W the initial phase structure of the wire is still martensite and no phase transformation occurs. The tensile loading had a little influence on the electrical resistance and had increased it only by a small fraction of approximately  $0.5\Omega$ . The test results of the wire when heated by pulses of 0.5W, 0.9W and 1.4W are absolutely different. Between heating pulses 0.24 W and 5.0 W, the NiTi wire undergoes an elastic deformation in the case of austenite causing the phase

structure of the wire to shift from martensite to austenite. This phase transformation greatly decreased the electrical resistance of the wire but, the tensile stress had a little influence on the electrical resistance and increased it by approximately  $0.5\Omega$ . A finding of possible significance is that the plots show an effect of tensile stress on the wire resistance, although it is very small. There is almost a linear increase with increase of stress and strain under tensile loading. However, the effect of phase transformation has greater influence on the wire resistance.

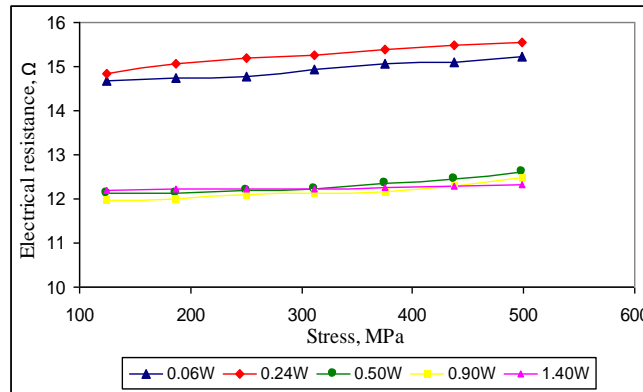


Fig. 9. Variation of NiTi electrical resistance during tensile loading in response to different heating pulses

From the experiment, it can be noted that the maximum force of 1.16 N applied on the wire can produce a change in magnitude of the generated error signal of 400 mV. Consequently, the effect of energizing the wire with higher demand keeping the same applied force will increase the value of this data character. Fig. 10 shows the magnitude of error signals as a function of the applied force at different heating pulses.

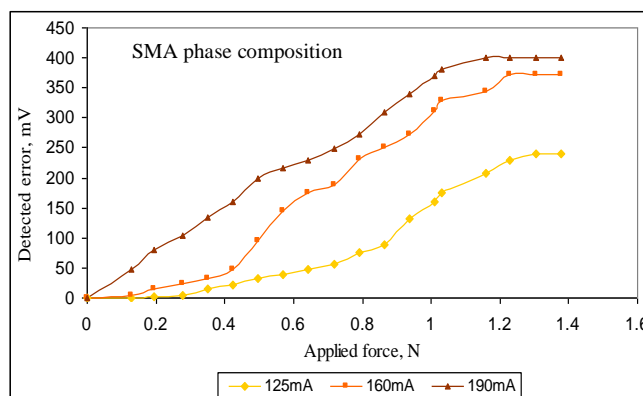


Fig. 10. Magnitude of error as a function of applied force at different heating pulses

## Conclusion

The oil bath test-rig developed in this work for the indirect temperature measurements has proved successful in getting accurate and reliable SMA wire temperatures with all its boundaries. It provided good results in accordance with many published data. It has been proved that it is meaningless and almost impossible to directly use a thermocouple to provide proper measurements of a very small wire diameter of  $100\mu\text{m}$ . It was shown that, martensite to austenite phase transformation takes place when the temperature of the SMA



element is between the austenite start  $A_s$  of 68 °C and the austenite finish  $A_f$  of 85 °C temperatures. Within this limit, phase transformation takes place whenever the distance between the temperature of the SMA element and the austenite finish  $A_f$  temperature decreases. Similarly, the austenite to martensite phase transformation takes place between the martensite start  $M_s$  of 65 °C and martensite finish  $M_f$  of 50 °C temperatures. The transformation takes place whenever the distance of the temperature of the SMA element and the martensite finish  $M_f$  temperature decreases. It is worth noting that these four transformation temperatures are stress dependent and therefore the effect of martensite ratio  $\zeta$  is considered in the phase transformation. Due to the highly non-linear behaviour of the SMA wire and the slow thermal response, hysteresis of 10-20 % was clear evident in many published curves in accordance with parameters related to temperature, displacement and resistance characteristics. If we consider the heating phase condition, we find there is a significant delay between the increase of the input heating current and the appearance of the force increase due to the integrating effect of the thermal mass of the wire. On the other hand, the descending phase show more causing far more pronounced hysteresis due to the slow cooling rate, so that temperature drops more slowly than heating current. Finally, we should emphasis that, all the work involved in this paper does not consider the dynamics of the SMA material in itself. Thus, it is not meant to physically predict the behaviour of the SMA element in time when the material is submitted to a constant stress. All our relations are algebraic relations in the involved quantities. i.e. temperature, resistance and neglecting the dynamics, which may provide a useful platform for further research.

## References

- [1] E. Darel, Hodson, Shape Memory Applications. Inc, Ming H. Wu, Memory Technologies, and Robert J. Biermann, Harrison Alloys, Inc.
- [2] H.M. Allam, "Single Element Based Tactile Display, " in Conf. Rec. June 2004 IEEE Int. Conf. Mechatronics, 7803-8599-3/04, Istanbul, Turkey.
- [3] H. M. Allam, "Development of Novel Tactile Displays Using Shape Memory Alloy," Ph.D. dissertation, Sch. Mech & Sys. Eng., Newcastle Univ., Newcastle, UK, 2005.
- [4] H.M. Alalem, "Convective Heat Transfer Model on Shape Memory Alloy (SMA) Actuator", WASET Int. Conf. Control, Automation, Robotics & Vision, DETC 2009 – 86536, Bangkok, December 2009.
- [5] Otsuka, Wayman, Shape Memory Materials. Cambridge University Press, 1998.
- [6] M. Mosley, C. Mavroidis, "Experimental Nonlinear Dynamic of a Shape Memory Alloy Wire Bundle Actuator," Journal of Dynamic Systems, Measurement, and Control, vol. 124/103, March. 2001.
- [7] <http://herkules.oulu.fi/isbn9514252217/html/x317.html>
- [8] P. M. Taylor, R. I. Davidson, I. P. Shutt, J.D .Ngu, H. M. Allam, " Prototype Interactive Tactile Array for C.A.D," 1<sup>st</sup> VR@P Int. Conf. Advanced Research in Virtual & Rapid Prototyping Portugal, 2003.
- [9] <http://www.picotech.com/datatable.html>
- [10] Micro-Epsilon, Non-Contact Optical Displacement Measuring System, Micro-Epsilon, Messtechnik, Germany.
- [11] H.M. Alalem, "Independent Control of Force & Displacement Using Shape Memory Alloy Tactile Display," ICMAS Int. Conf. Applied Mechanics and Materials Vols. 789-790 (2015) pp 972-981© (2015) Trans Tech Publications, Switzerland, 2015.